International Journal of Progressive Sciences and Technologies (IJPSAT)
ISSN: 2509-0119.

http://ijpsat.ijsht-journals.org
Vol. 30 No. 2 January 2022, pp. 636-643

Resistance Analysis of a Hydrofoil Fast Patrol Boat Using Computational Fluid Dynamics

Gerard Richard Latuhihin[1], Johanna Matakupan[2], Fella Gaspersz[3], Richard Benny Luhulima[4]

[1,2,3,4] Department of Naval Architecture

Faculty of Engineering, Universitas Pattimura

Ambon, Indonesia

***Abstract*— As an archipelago, Indonesia needs a comprehensive national fleet of ships to retain sovereignty to defend and protect Indonesian waterways. Indonesia's open seas are bordered by international waterways, making them vulnerable to foreign threats. Thus, warships that serve as coastal patrol boats of varied sizes are required depending on the task and assignment. The main feature of patrol boats is speed, which is achieved through reducing the ship's resistance. Hydrofoils are now being used on ships owing to their benefits, such as minimizing the resistance created by the lift (lift) that elevates the hull above the water, thereby reducing the area of resistance caused by the drag force between the submerged hulls of the ship. The goal of this research was to see how adding hydrofoil to the ship's hull affected the ship's resistance. The impact of employing hydrofoils on rapid patrol boats was studied using Computational Fluid Dynamics. This research compared resistance on fast patrol boats with and without hydrofoils to optimize ship resistance. The use of Foil 4712 on a Hydrofoil can produce the optimum lift in foilborne conditions at Froude number 1.0 where Fast Patrol Boat without foil produces a drag of 953kN and Fast Patrol Boat with Foil produces a drag of 856 kN. Then, the Foil is able to reduce resistance by about 13% at Fr = 1.2 it gives the advantage that the installation of Foil is quite good at high speeds.**

***Keywords*—Fast Patrol Boat, Hydrofoil, Resistance, CFD.**

I. INTRODUCTION

As a sovereign archipelago republic with a large open sea region linked to international waterways, Indonesia's outer waters are at risk of war owing to threats and security disruptions from a variety of external interests. The three Indonesian Territorial waters Sea Lanes link Indonesia's geostrategic zone to international seas, as seen in Figure 1. A national fleet of ships, including battleships and patrol boats, is required to preserve sovereignty and safeguard all territorial seas under national control, including areas off the border[1].

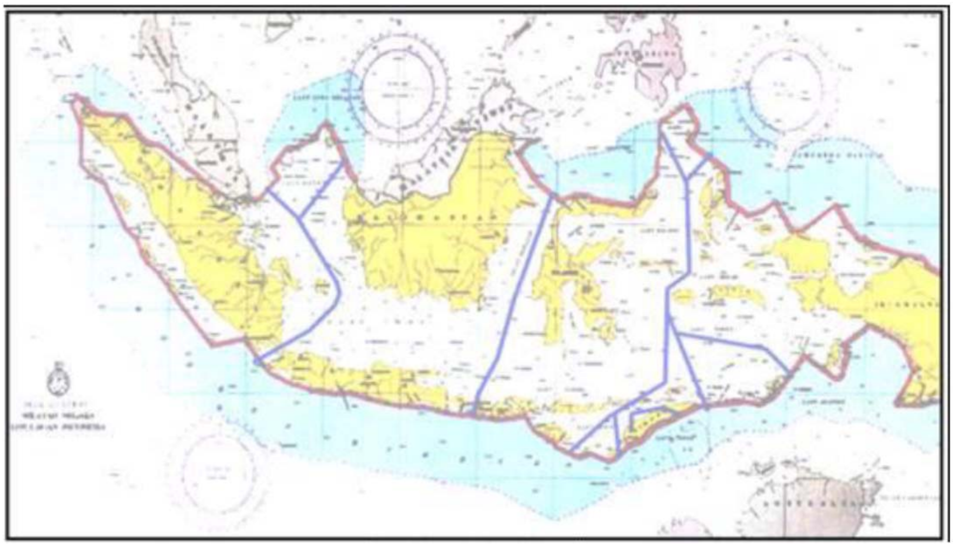

Figure 1. Map of the Geostrategic Region of the Republic of Indonesia with 3 ALKI Lines from North-South

Appropriate ship conditions are required to support patrol boats doing strategic and clandestine missions. A patrol boat's speed is critical. Numerous advancements and breakthroughs in maritime technology have enabled the use of hydrofoils to minimize ship drag and increase ship speed. The use of hydrofoils on ships has several advantages, including lowering the resistance generated by the lifting force that elevates the hull above the water and lowering the area of resistance caused by friction between the ship's submerged hull[2].

One technique to maximize energy and hull consumption is to use fast boat technologies that reduces ship resistance. Ships that travel at high speeds can benefit from hydrodynamic lift to lower hull resistance because it can minimize the amount of wet surface area that is directly related to hull resistance. At low speeds, the buoyancy point is the most important factor. A fast ship's hydrodynamic pressure lifts around 85% of the ship's weight at its lowest operating speed. Depending on the ship's speed, hydrodynamic pressure forces create a horizontal angle known as the trim angle (τ) on the vessel[3].

The hull spreads above the surface of the water. When the hull begins to lift from the water and the ship's weight is supported by the foil in order to reduce the area of resistance created by the frictional force between the submerged hull and the water, the foil has the effect of increasing the ship's lift when speed is added. After the hull is lifted to its maximum extent from the water, the required lift is constant. A hydrofoil on board is weight-sensitive and must be operated at a relatively high speed to generate the required dynamic lift force to support the weight with the appropriate foil size[4].

The majority of hydrofoil ships have a unique strut-foil system compared to other hydrofoil ships. Essentially, there are two types of foil systems: surface piercing foil and completely submerged foil. If the front foil supports 65 percent or more of the ship's weight, it is classified as conventional; if the front foil supports 65 percent or more of the ship's weight, it is classified as canard; and if the ship's weight is distributed fairly evenly between the front and rear foils, it is classified as tandem[5].

The purpose of this research was to determine the effect of using hydrofoils on rapid patrol boats on eliminating impediments. To optimize ship resistance, this study analyzed the barriers encountered by fast patrol boats without a hydrofoil and those encountered by fast patrol boats installed with a hydrofoil.

II. METHODS

A. Modelling

The research was conducted on fast patrol boat as shown in Figure 1. Furthermore, the Fast Patrol Boat model was analyzed for CFD simulation at Fr=0.5 – 1.2 The geometry parameters of the trimaran hull are presented in Table 1.

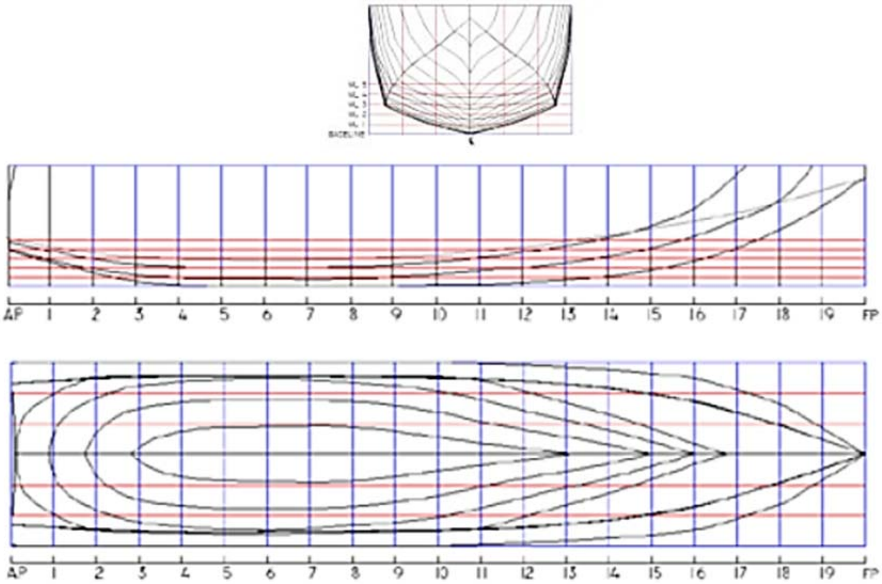

Figure 2 Lines plan of fast patrol boat

(a) (b)

Figure 3(a) Fast Patrol Boat without Hydrofoil; (a) with Hydrofoil

Tabel 1 Parameter Dimension of Model

Parameter	Unit	**Boat**
L_{OA}	m	14.45
L_{WL}	m	12.93
B	m	3.4
T	m	0.65
Wetted Surface Area	m^2	35,33
Displacement	kg	12.36
Block Coefficient (C_B)		0.467

B. Governing Equation

A three-dimensional equation created and utilized in the CFD model is the Reynolds-averaged Navier-Stokes (RANS) technique. Incompressible flow equations created by ANSYS-CFX software are used to address flow issues in ship walls. For incompressible flows, the averaged continuity and momentum equations are provided in the following two equations [6]. In Equations (1) and (2), the mass and momentum equations are expressed as follows:

$$\frac{\partial \rho}{\partial t} + \nabla.(\rho U) = 0 \quad (1)$$

$$\frac{\partial(\rho U)}{\partial t} + \nabla.(\rho U \; x \; U) = -\nabla p + \nabla.\tau + S_M \quad (2)$$

where the stress tensor, τ is related to the strain rate.

Furthermore, Reynolds Averaged Navier-Stokes (RANS) was developed, which is a variation of unstable Navier-Stokes incorporating averaged and fluctuating parameters. Anderson [7] defines the turbulence model based on the RANS equation as a statistical turbulence model produced by the statistical average method used to derive the equations. The average equations of RANS are provided in Equations (3) and (4):

$$\frac{\partial \rho}{\partial t} + \frac{\partial}{\partial x_j}\left(\rho U_j\right) = 0 \quad (3)$$

$$\frac{\partial(\rho U)}{\partial t} + \frac{\partial}{\partial x_j}\left(\rho U_i U_j\right) = -\frac{\partial p}{\partial x_j} + \frac{\partial}{\partial x_j}\left(\tau_{ij} - \overline{\rho u_i u_j}\right) + S_M \quad (4)$$

where τ is the stress tensor molecular consisting of normal and shear stress components

The near-wall performance of the k- ω appealing model may be employed without the possibility of causing inconsistencies to its free stream sensitivity, and it provides highly precise predictions of the start and magnitude of flow separation under undesirable pressure gradients [8]. The SST model has benefited greatly from the strength of the fundamental turbulence model, which is why the development of an accurate and dependable near-wall formulation of the Wilcox model has greatly aided its industrial application of turbulence, heat, and mass transport.

C. Boundary Conditions

The most often recommended computational domain for simulating at a velocity intake was placed 2L ahead perpendicular to the front and a pressure outlet of 5L toward the back, also perpendicularly. The transverse and vertical directions were both set atin order to counteract the effects of transverse pressure [9]. In order to prevent backflow, Ford and Winroth [10] implemented a pressure exit outflow for the downstream boundary condition, as illustrated at Figure 4.

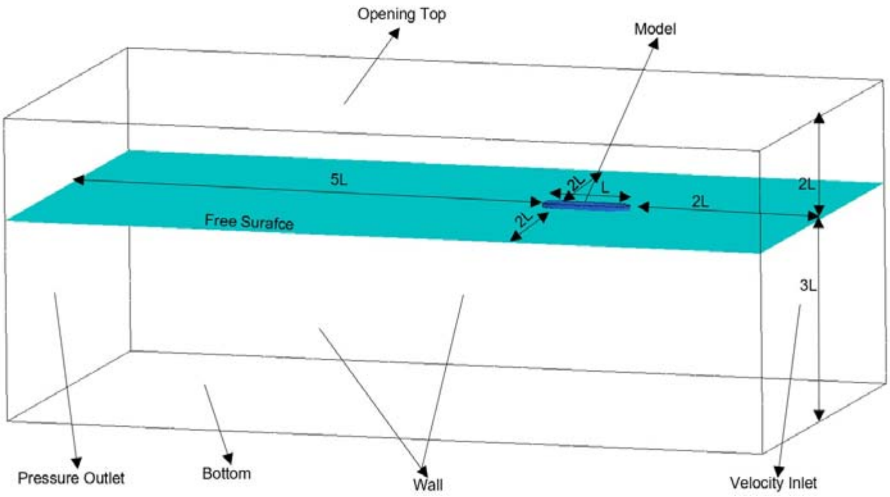

Figure 4 Boundary Conditions

D. **Grid Independence**

The use of an unstructured mesh in any part of grid creation offers a number of benefits over using a structured mesh. The use of an inflation mesh enables the CFD to correctly complete flow along the model's wall by characterizing the flow separation near the hull of the model [11], as shown at Figure 5.

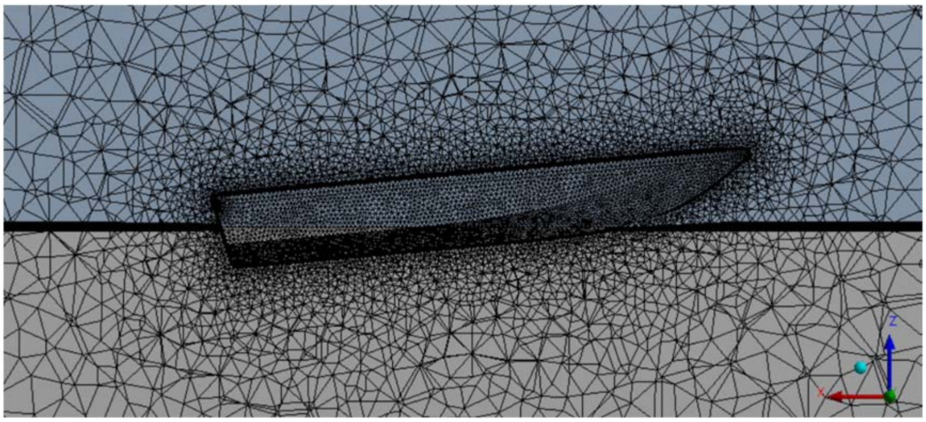

Figure 5 Unstructed with inflation mesh model

Consistency and history records that represent the working period of a variable amplitude deviation comprehensive approach to CFD simulation are critical aspects of the numerical simulation calculation. Convergence and history records are important aspects of the numerical simulation calculation. The root-mean-square (RMS) criterion was employed to verify for convergence, with the residual target value (variable value) approaching 10^{-4} and the results given in Figure 6(a) indicating that the model is in fact converging. A well-posed issue and a closely converging solution are indicated by the presence of monotonic convergence in these residual monitors. Accurate findings are directly correlated to the quantity of cells or grids used in calculations. A project plan in which the number of meshing is determined independently was used in the illustration as shown in Figure 6 (b). Simulation grid independence of Trimaran A with Fr = 0.3 was conducted. Results obtained from grid independence tests indicated that with total resistance coefficient of 0.098 to optimum difference C_T of 1.02 percent, where trimaran model simulations on grid number 1,698,532 are the best.

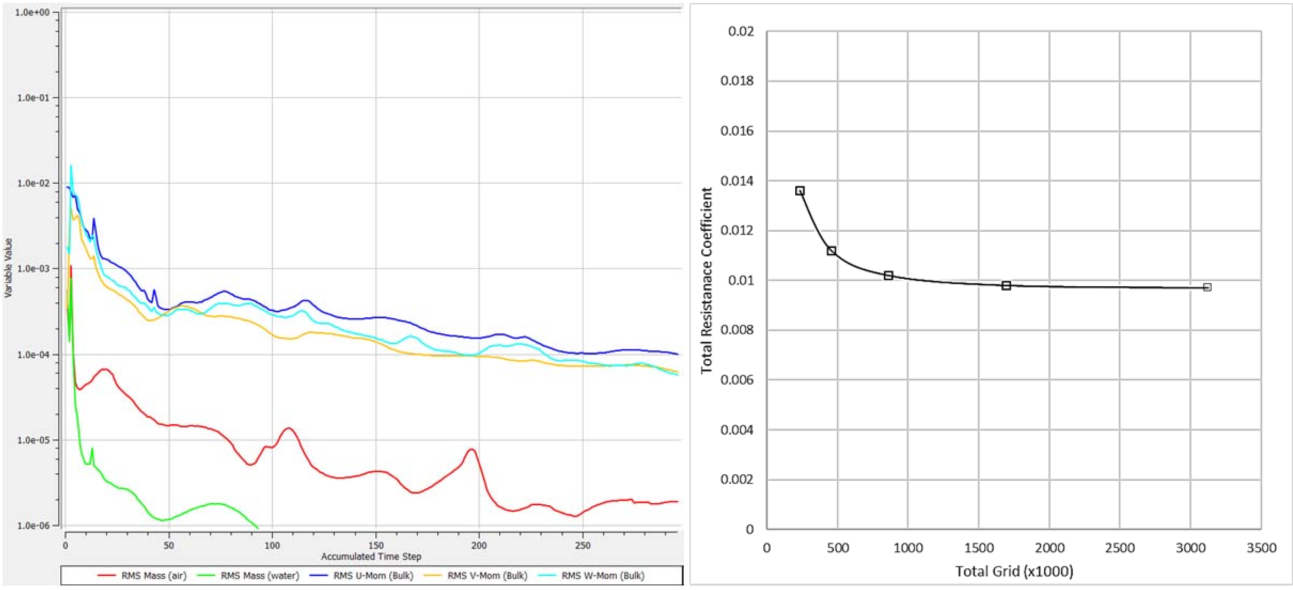

(a) (b)

Figure 6 (a) Covergency; (b) Grid Independence Study

III. Result and discussion

Ship resistance analysis using the fast boat test model without and with a hydrofoil. Simulations are carried to determine the lift and drag of fast boats. Thus, the lift, drag, and lift/drag ratios for the three variations of the foil laying model at froude numbers 0.3 to 1 are obtained. With the draft and displacement conditions of the hydrofoil fast boat considered constant in all conditions, the froude number value is determined by the length of the water line (LWL). The ship is assumed same in all variations of the froude number, which means that the change in draft caused by the lift generated by each variation in speed/froude number was not factored into the test. The Fast Patrol Vessel Calculation Results are provided in Figure 7

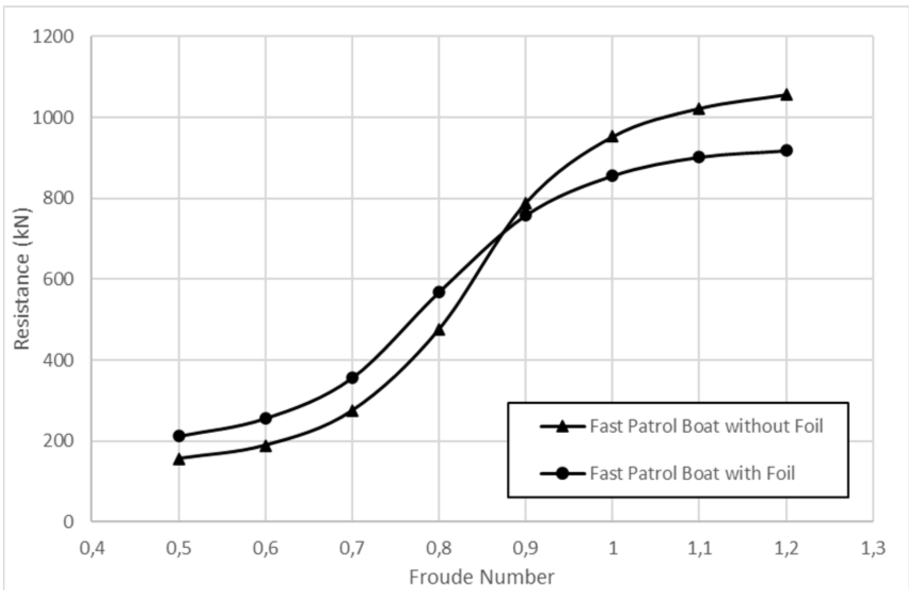

Figure 7 Fast Patrol Boats Resistance using CFD

It can be seen in Figure 7 that the results of the hydrofoil fast boat test indicate that there is a hump area in the vicinity of the froude number of 0.90. In fast boats with a planning hull type hull between froude numbers 0.55 and 0.85, a phenomenon known as the hump area may occur during the transition from displacement mode to planning mode, which is also known as semi-planning mode, and can be seen [12]. Similarly, as seen in figure 8, this is explained.

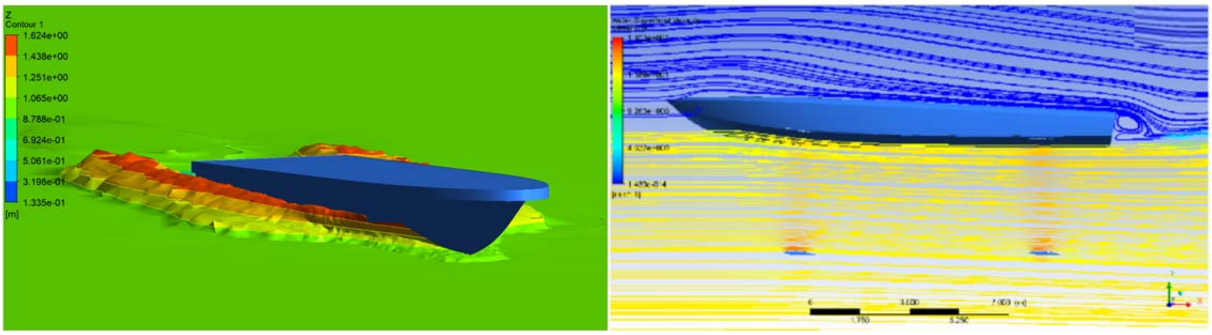

(a) (b)

Figure 8 Contour and Streamline visualization of (a) Fast Patrol Boat without Hydrofoil; (a) with Hydrofoil

It is not just fast patrol boats with hydrofoils that face substantial hump drag; fast patrol boats without hydrofoils also suffer from significant hump drag. According to test findings obtained using CFD, the hump area phenomena occur on hydrofoil fast boats between the numbers 0.9 and 1.0. In addition, this occurs in fast boats without a hydrofoil when the froude numbers are between 0.80 and 0.01 (which correspond to the transition phase from displacement mode to planning mode) .

IV. CONCLUSION

Calculations using CFD software can be performed on the hydrofoil fast boat model because the results obtained can be used to analyze the lift force and drag force of the foil system. Even by using CFD Software, the difference in lift force generated by the front and rear foils can be known. The conclusions from the tests carried out are as follows:

1. The turbulence model used in testing the hydrofoil fast boat is the SST turbulence model (k-omega SST).
2. The use of Foil 4712 on a Hydrofoil can produce the optimum lift in foilborne conditions at Froude number 1.0 where Fast Patrol Boat without foil produces a drag of 953kN and Fast Patrol Boat with Foil produces a drag of 856 kN.
3. The use of Foil is able to reduce resistance by about 13% at Fr = 1.2 it gives the advantage that the installation of Foil is quite good at high speeds.
4. At low speed with Fr=0.5, Foil Installation has a negative impact with an additional resistance of 35.9%
5. Use/Installation of Foil really needs to be considered at the operational speed of the ship.

ACKNOWLEDGMENT

The authors would like to express our gratitude to Universitas Pattimura as well as all other parties that have also contributed to the successful completion of this research.

REFERENCES

[1] B. Suseto, Z. Othman, and F. M. Razalli, “The need to reform Indonesia’s maritime strategy: A review,” *Indones. J. Geogr.*, vol. 50, no. 2, pp. 145–154, 2019, doi: 10.22146/ijg.27954.

[2] O. M. Faltinsen, *Hydrodynamics of High-Speed Marine Vehicles*. Cambridge: Cambridge University Press, 2006.

[3] T. C. Fu, R. Akers, T. O’Shea, K. Brucker, D. G. Dommermuth, and E. Lee, “Measurements and computational predictions of a deep-V monohull planing hull,” in *11th International Conference on Fast Sea Transportation, FAST 2011 - Proceedings*, 2011.

[4] I. Kumagai, Y. Takahashi, and Y. Murai, “Power-saving device for air bubble generation using a hydrofoil to reduce ship

drag: Theory, experiments, and application to ships," *Ocean Eng.*, 2015, doi: 10.1016/j.oceaneng.2014.11.019.

[5] K. Suastika, A. Hidayat, and S. Riyadi, "Effects of the application of a stern foil on ship resistance: A case study of an Orela crew boat," *Int. J. Technol.*, vol. 8, no. 7, pp. 1266–1275, Dec. 2017, doi: 10.14716/IJTECH.V8I7.691.

[6] J. H. Ferziger and M. Perić, *Computational Methods for Fluid Dynamics*. Berlin, Heidelberg: Springer Berlin Heidelberg, 2002.

[7] J. D. Anderson, *Computational Fluid Dynamics: The Basics with Applications*. New York, USA. pp. 526-532: McGraw-Hill, 1995.

[8] F. R. Menter, "Two-equation eddy-viscosity turbulence models for engineering applications," *AIAA J.*, vol. 32, no. 8, pp. 1598–1605, Aug. 1994, doi: 10.2514/3.12149.

[9] A. G. Elkafas, M. M. Elgohary, and A. E. Zeid, "Numerical study on the hydrodynamic drag force of a container ship model," *Alexandria Eng. J.*, vol. 58, no. 3, pp. 849–859, Sep. 2019, doi: 10.1016/j.aej.2019.07.004.

[10] C. L. Ford and P. M. Winroth, "On the scaling and topology of confined bluff-body flows," *J. Fluid Mech.*, 2019, doi: 10.1017/jfm.2019.583.

[11] ANSYS, *ANSYS CFX-Solver Theory Guide*. Canonsburg, PA, USA: Ansys Inc, 2020.

[12] R. Yousefi, R. Shafaghat, and M. Shakeri, "Hydrodynamic analysis techniques for high-speed planing hulls," *Appl. Ocean Res.*, vol. 42, pp. 105–113, Aug. 2013, doi: 10.1016/j.apor.2013.05.004.